SMOKE AND FLAME TEMPERATURE PROPAGATION CHARACTERISTICS DURING CABIN FIRE IN AIRBUS A380

Tian-Qi LIU*, Ke-Nan LIU, Rui-heng JIA

College of Safety Engineering, Shenyang Aerospace University, Shenyang, China

* Corresponding author: Tian-Qi LIU; E-mail: liutianqi613@163.com

The Airbus A380 cabin is selected as the research object to study the smoke and temperature propagation process of upper cabin fires. The results show that during the fire, the overall spread of smoke lasted for 600 s. At z=3.6 m in the upper cabin aisle, the time required for smoke propagation in first class, business, and luxury economy cabins is 89 s, 59 s, and 83 s. At z=3.6 m in the upper cabin seats, the time required for smoke propagation in first class, business, and luxury economy cabins is 89 s, 82 s, and 106 s. The closer the cabin is to the front of the first class cabin, the higher the temperature, while the closer the business cabin is to the fire source, the higher the temperature. In the upper cabin aisle and seats, the temperature in first class, business class, and luxury economy class is higher as it gets closer to the fire source. The ranking of comprehensive danger level from low to high is luxury economy class, first class, and business class.

Key words: *Airbus A380; smoke propagation; flame temperature; numerical simulation*

1. Introduction

In modern civil aircraft transportation, flight safety has become a global concern, and fires in aircraft cabins and personnel evacuation after a fire have become important issues of concern in the transportation process of civil aircraft. If an aircraft catches fire during flight or is about to take off without timely and rapid evacuation of personnel, it will not only cause significant economic losses, but may also lead to serious consequences such as aircraft damage and fatalities [1]. With the continuous progress of the global aviation industry, the prevention of civil aircraft fires has become particularly important. The occurrence of cabin fires in aircraft can further lead to circuit failures, fuel leaks, and other issues in the cabin, which can affect the normal flight of the aircraft and result in tragic aircraft crashes and fatalities [2,3]. According to investigation reports on past aircraft accidents, cabin fires were a major cause of aircraft accidents. Although the relevant departments have taken many preventive measures against cabin fires, there is still a significant risk of fire occurring inside the aircraft cabin.

In the research results of aviation safety, the process of cabin fire propagation and the evacuation characteristics of cabin personnel have received attention. In the case of flight failure, there may be obvious pressure changes in the aircraft cabin. Therefore, research results on the characteristics of aircraft fire propagation under different pressure conditions have been reported. The research found that the smaller the pressure in the cabin, the greater the flame propagation distance [4-

7]. At the same time, the radiant flux of the flame will increase with the increase of the flame propagation time [8,9]. However, further research has shown that when the pressure inside the cabin decreases to a specific value, a portion of the flame inside the cabin will actually extinguish, which may be due to insufficient local oxygen supply for sustained flame combustion in a short period of time [10]. When the pressure inside the cabin decreases, the high-temperature area of flame propagation inside the cabin will increase, thereby increasing the contact time between the high-temperature flame and cabin materials. If the liner of the cabin is ignited, the toxic and harmful gases and smoke generated will increase the mortality rate of accidents [11-15].

The combustion characteristics of combustible materials in the cabin are of great concern. Related studies have reported the pyrolysis characteristics of composite materials in the cabin [16], and analyzed the mass loss characteristics of carbon fiber epoxy resin in high-temperature environments [17]. In terms of emergency evacuation of cabin personnel, relevant studies have shown that simulating the evacuation process can provide important references [18,19]. The theoretical model of personnel evacuation has been continuously optimized [20,21], and the reliability of the mathematical model of personnel evacuation has been verified by experiments [22-24]. Research has found that during the personnel evacuation process of subway stations, stairwells are the most prone location for personnel congestion [25]. For high-rise buildings, the research has found that people tend to choose the nearest exit when escaping. If there are more people in the building, the crowding phenomenon near the exits on lower floors will last longer, which can lead to a decrease in evacuation rate [26]. In summary, the current research on the propagation characteristics of aircraft fires mainly focuses on the combustion performance and flame structure of cabin materials.

This article analyzes the smoke propagation characteristics and temperature propagation laws of Airbus A380 cabin fires. Through fire simulation, the propagation process of aircraft cabin fires can be conveniently restored, and the smoke concentration and temperature changes at different positions and heights in the cabin can be intuitively obtained. The research results can provide scientific reference for the layout of fire prevention and extinguishing facilities in the cabin and the formulation of personnel evacuation plans, while also improving the safety performance of aircraft and the success rate of personnel evacuation. In addition, studying the propagation laws of aircraft fires can provide scientific theoretical support for the design and improvement of aircraft cabin layout, reduce the occurrence of fires, and improve the overall safety performance of the aircraft.

2. Establishment and reliability testing of cabin fire models

2.1. Simulation principle and method

When a fire occurs in an aircraft cabin, the equations in the flow field are very complex, it is impossible to obtain accurate solutions for various parameters in the flow field. Therefore, Pyrosim software can divide the cabin into many small geometric units. Based on the conservation equations and turbulent combustion equation, numerical methods are used to solve the fire mathematical model. The discrete flow field characteristics are summarized to obtain the fire characteristics of the entire cabin. For turbulent combustion and turbulent flow phenomena in the cabin, Pyrosim can calculate the propagation process of fire based on the material characteristics of combustible materials. The gas-phase turbulence model during combustion is the k-ε model. The combustion model selected is the vortex dissipation model. The components of smoke include solid particles, CO, CO_2, H_2O, and H_2.

The energy conservation equation used in numerical simulation is as follows.

$$\frac{\partial \rho T}{\partial t} + \mathrm{div}\left(\rho \vec{u} T\right) = \mathrm{div}\left(\frac{k}{c_p}\mathrm{grad}T\right) + S_T$$

Where, ρ is the fluid density, kg/m^3; t is the time, s; $\vec{u}$ is the velocity vector, m/s; c_p is the specific heat capacity, J/(kg·°C); T is the temperature, °C; k is the heat-transfer coefficient, W/(m^2·°C); S_T is the viscous dissipation term.

2.2. Establishment of cabin geometric model

The Airbus A380 is the world's largest ultra wide body passenger aircraft manufactured by European Airbus, with a cabin length of 56.5 m, width of 6.7 m, and height of 4.9 m. The upper and lower cabin heights are both 2.3 m, and the cabin floor thickness is 0.3 m. The maximum passenger capacity is 520 people. The overall layout of the cabin is shown in fig. 1. The arrangement of seats is arranged according to the third class cabin, which is divided into first class, business class, and economy class. There are 8 first-class seats, 56 business class seats, and 73 luxury economy class seats in the upper cabin, with a total of 27 rows of seats. The lower cabin is all economy class, with a total of 383 seats and 41 rows of seats. The aisle widths for first class, business class, luxury economy class, and economy class are 1.53 m, 1.01 m, 0.97 m, and 0.86 m, respectively. The seat widths for first class, business class, and economy class are 0.55 m, 0.55 m, and 0.47 m, respectively. Pyrosim software was used to construct a 1:1 geometric model of the Airbus A380 aircraft cabin. The walls on both sides of the cabin are curved, with luggage racks above the seats. X, Y, and Z coordinate axes are constructed. The cabin is 6.7 m wide in X direction, 4.9 m high in Z direction, and 56.5 m long in Y direction.

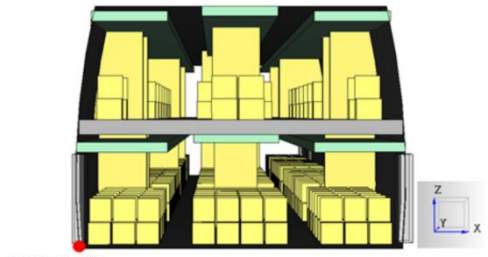

Figure 1. Front view of double decker cabin (XOZ direction)

On the basis of establishing the cabin model, polyurethane is set as the combustible material that causes the fire. It is a commonly used waterproof material on airplanes, and the fire source size is 0.2 m×0.2 m×0.1 m. The fire source was set in a densely populated area, namely the middle of the upper cabin. The location of the fire source is shown in fig. 2, and the center coordinates of combustibles are (3.29, 28.95, 3.05). The maximum heat release rate of the fire source is 3000 kW/m^2.

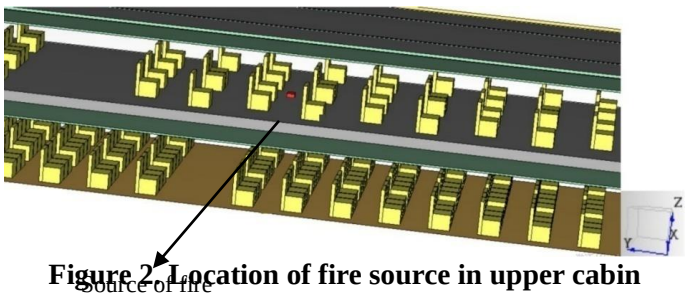

Figure 2. Location of fire source in upper cabin

To analyze the smoke concentration and temperature changes during different periods of fire, corresponding temperature and smoke monitoring points are set up. When walking upright, the height of the breathing belt is 1.5 m, and when bending down, the height of the breathing belt is 1 m. Therefore, in order to clearly and intuitively analyze the smoke diffusion and temperature changes inside the upper cabin after a fire, monitoring points are evenly distributed at the upper cabin aisle and seat positions according to the two heights of normal upright walking and bending forward. Monitoring points are set along the Y direction at the bending and standing breathing belt heights z=3.6 m and z=4.1 m in the upper cabin aisle x=2.1 m and seat x=3.35 m planes. The specific names and locations of monitoring points are shown in tab. 1.

Table 1. Name and location of monitoring points

name	position	name	position	name	position	name	position
1	(1.94,0,3.6)	31	(3.29,0,3.6)	61	(1.94,0.15,3.6)	91	(3.29,0.15,3.6)
2	(1.94,4,3.6)	32	(3.29,4,3.6)	62	(1.94,4.15,3.6)	92	(3.29,4.15,3.6)
3	(1.94,8,3.6)	33	(3.29,8,3.6)	63	(1.94,8.15,3.6)	93	(3.29,8.15,3.6)
4	(1.94,14,3.6)	34	(3.29,14,3.6)	64	(1.94,14.15,3.6)	94	(3.29,14.15,3.6)
5	(1.94,18,3.6)	35	(3.29,18,3.6)	65	(1.94,18.15,3.6)	95	(3.29,18.15,3.6)
6	(1.94,22,3.6)	36	(3.29,22,3.6)	66	(1.94,22.15,3.6)	96	(3.29,22.15,3.6)
7	(1.94,26,3.6)	37	(3.29,26,3.6)	67	(1.94,26.15,3.6)	97	(3.29,26.15,3.6)
8	(1.94,30,3.6)	38	(3.29,30,3.6)	68	(1.94,30.15,3.6)	98	(3.29,30.15,3.6)
9	(1.94,32,3.6)	39	(3.29,32,3.6)	69	(1.94,32.15,3.6)	99	(3.29,32.15,3.6)
10	(1.94,36,3.6)	40	(3.29,36,3.6)	70	(1.94,36.15,3.6)	100	(3.29,36.15,3.6)
11	(1.94,40,3.6)	41	(3.29,40,3.6)	71	(1.94,40.15,3.6)	101	(3.29,40.15,3.6)
12	(1.94,44,3.6)	42	(3.29,44,3.6)	72	(1.94,44.15,3.6)	102	(3.29,44.15,3.6)
13	(1.94,48,3.6)	43	(3.29,48,3.6)	73	(1.94,48.15,3.6)	103	(3.29,48.15,3.6)
14	(1.94,52,3.6)	44	(3.29,52,3.6)	74	(1.94,52.15,3.6)	104	(3.29,52.15,3.6)
15	(1.94,56,3.6)	45	(3.29,56,3.6)	75	(1.94,56.15,3.6)	105	(3.29,56.15,3.6)
16	(1.94,0,4.1)	46	(3.29,0,4.1)	76	(1.94,0.15,4.1)	106	(3.29,0.15,4.1)
17	(1.94,4,4.1)	47	(3.29,4,4.1)	77	(1.94,4.15,4.1)	107	(3.29,4.15,4.1)
18	(1.94,8,4.1)	48	(3.29,8,4.1)	78	(1.94,8.15,4.1)	108	(3.29,8.15,4.1)
19	(1.94,14,4.1)	49	(3.29,14,4.1)	79	(1.94,14.15,4.1)	109	(3.29,14.15,4.1)
20	(1.94,18,4.1)	50	(3.29,18,4.1)	80	(1.94,18.15,4.1)	110	(3.29,18.15,4.1)
21	(1.94,22,4.1)	51	(3.29,22,4.1)	81	(1.94,22.15,4.1)	111	(3.29,22.15,4.1)
22	(1.94,26,4.1)	52	(3.29,26,4.1)	82	(1.94,26.15,4.1)	112	(3.29,26.15,4.1)
23	(1.94,30,4.1)	53	(3.29,30,4.1)	83	(1.94,30.15,4.1)	113	(3.29,30.15,4.1)
24	(1.94,32,4.1)	54	(3.29,32,4.1)	84	(1.94,32.15,4.1)	114	(3.29,32.15,4.1)
25	(1.94,36,4.1)	55	(3.29,36,4.1)	85	(1.94,36.15,4.1)	115	(3.29,36.15,4.1)
26	(1.94,40,4.1)	56	(3.29,40,4.1)	86	(1.94,40.15,4.1)	116	(3.29,40.15,4.1)
27	(1.94,44,4.1)	57	(3.29,44,4.1)	87	(1.94,44.15,4.1)	117	(3.29,44.15,4.1)
28	(1.94,48,4.1)	58	(3.29,48,4.1)	88	(1.94,48.15,4.1)	118	(3.29,48.15,4.1)
29	(1.94,52,4.1)	59	(3.29,52,4.1)	89	(1.94,52.15,4.1)	119	(3.29,52.15,4.1)
30	(1.94,56,4.1)	60	(3.29,56,4.1)	90	(1.94,56.15,4.1)	120	(3.29,56.15,4.1)

2.3. Reliability test of fire numerical simulation

To verify the feasibility of the simulation results of the Airbus A380 cabin fire in this article, the cabin fire experimental data and simulation data were compared and analyzed. In 1982, researchers conducted an aircraft fire flammability test using a passenger plane, which was conducted at an ambient temperature of 21 ℃ [27]. The fire source of combustion experiment is set under the aircraft seat, and the material of the aircraft seat is polyurethane foam. Input the various parameters in the experiment into Pyrosim, so that the parameters in the experiment are the same as those in the simulation process, so that the simulation environment is close to the real experimental environment. This article compares the temperature data obtained 60 seconds after a fire with the simulated temperature data, and the comparison results are shown in fig. 3.

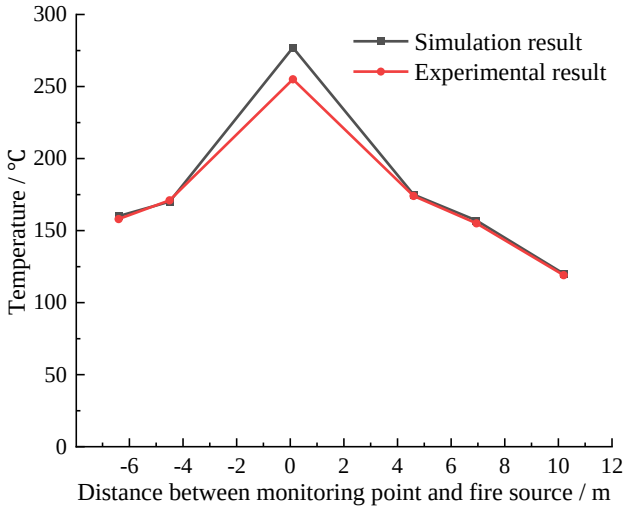

Figure 3. Experimental and simulation results of cabin flame temperature

By comparing the combustion experiments and simulated temperature data of the Airbus A380 aircraft cabin, it can be found that there is a certain degree of error in the temperature data at the fire source, with an error rate of 6.8%. This is because Pyrosim software will perform unstable calculations on the average absorption coefficient and temperature near the fire source during numerical analysis, and intermittent flames will cause significant instantaneous temperature fluctuations. The trend of experimental data and simulation data at other locations is basically consistent, proving the feasibility of conducting fire simulation research in this paper.

3. Smoke and flame temperature propagation characteristics in Airbus A380 cabin fire

3.1. Smoke spreading characteristics at different times during cabin fires

The smoke spread process at different times during the upper cabin fire of Airbus A380 is shown in fig. 4. The red circle represents the location of the fire, and *t* represents the time after the fire occurred, with the unit being s. Analysis shows that smoke starts to appear from 3 s, and from 3 s to 8 s is the stage of rapid smoke rise. Due to the effects of smoke plumes and thermal buoyancy, the smoke reaches the ceiling of the upper cabin in a very short time. From 8 s to 73 s, the smoke in the upper cabin began to sink. When the smoke touched the sidewall, it spread downwards along the sidewall, and the smoke sank slower at the top of the fire source than at other positions, forming an

umbrella shaped smoke layer. At 77~82 s, the smoke in the upper cabin began to spread downwards. At 77~82 s, the smoke spread downwards from the stairs, and at 82 s, the smoke spread more noticeably downwards from the stairs. At 77~600 s, the smoke in the upper cabin begins to backflow; From 82 s to 600 s, smoke gradually spread in the lower cabin, and the entire process lasted until 600 s. Both upper and lower cabins were covered by smoke.

Figure 4. Spread process of cabin smoke at different times

3.2. Smoke spreading characteristics at different positions during cabin fires

3.2.1 Smoke spreading characteristics at the upper cabin aisle

The monitoring point for the height of the person bending forward is selected, which is the monitoring point at a height of z=3.6 m, to detect the unit length opacity data of smoke in the upper cabin aisle. The opacity of smoke per unit length is positively correlated with the mass fraction of smoke around the monitoring point. As shown in fig. 5, the smoke spread rate is highest at the head position of the first-class cabin. In the business cabin, the smoke propagation rate at monitoring point

8 is the highest, and the duration increases with the distance from the fire source. The smoke propagation rate is highest at the rear of the luxury economy class cabin, and the duration increases with the distance from the rear of the cabin. The shortest time for the smoke unit length opacity rate to reach 100%/m in first class, business class, and luxury economy class is 89 s, 59 s, and 83 s, respectively. Therefore, at an altitude of z=3.6 m, the ranking of danger level from low to high is luxury economy class, first class, and business class.

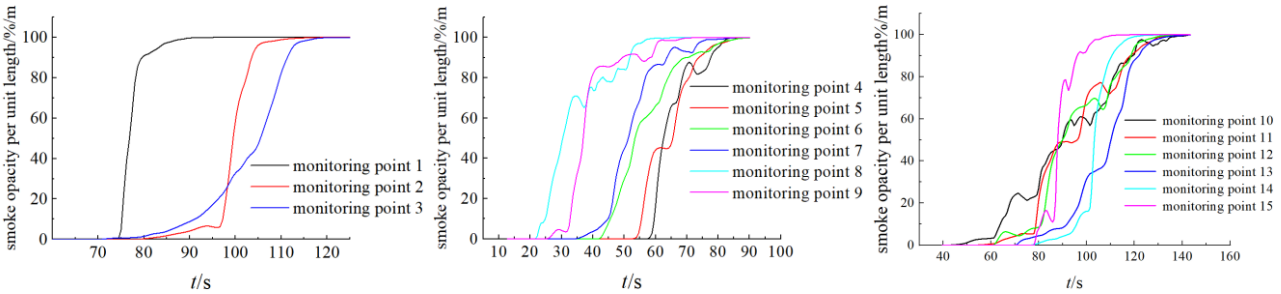

(a) First class (b) Business class (c) Luxury economy class

Figure 5. Data from smoke monitoring points at z=3.6 m in the upper cabin aisle

The monitoring points with a walking height of z=4.1 m are selected to monitor the smoke changes in the upper cabin aisle. The results are shown in fig. 6. In first class and business class, the time and rate of smoke propagation depend on the distance between the monitoring point and the fire source, respectively. This pattern is different from the height of the breathing belt when a person bends down and moves forward. The shortest time for the unit length of smoke to increase the opacity to 100%/m is 89 s for first class cabin, 68 s for business cabin, and 106 s for luxury economy cabin. Under the condition of z=4.1 m altitude, the ranking of comprehensive danger level from low to high is luxury economy class, first class, and business class.

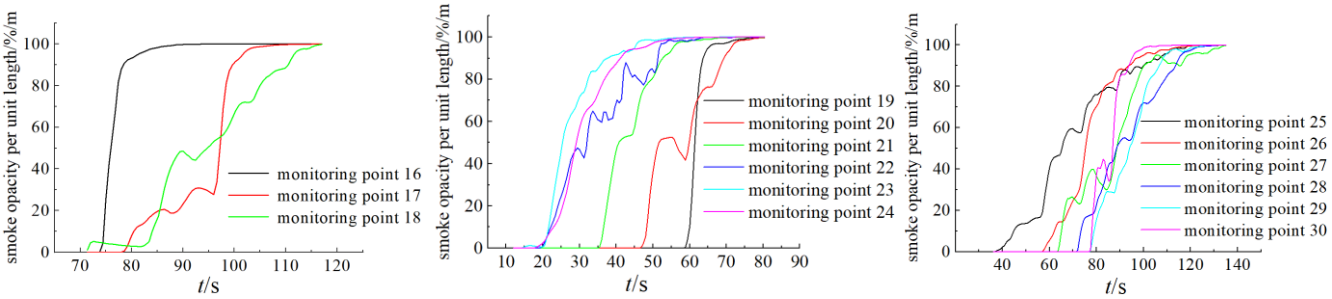

(a) First class (b) Business class (c) Luxury economy class

Figure 6. Data from smoke monitoring points at z=4.1 m in the upper cabin aisle

3.2.2 Smoke spreading characteristics at upper cabin seats

The monitoring point with a height of z=3.6 m are selected to monitor the smoke changes at the upper cabin seats, as shown in fig. 7. The time for smoke diffusion depends on the distance from the front of the cabin in first-class class, the distance from the fire source in business class, and the distance from the rear of the cabin in luxury economy class. The time for smoke transmission in first-class, business class, and luxury economy class is 89 s, 82 s, and 106 s, respectively. Under the condition of z=3.6 m, the comprehensive hazard level ranks from low to high in luxury economy class, first class, and business class.

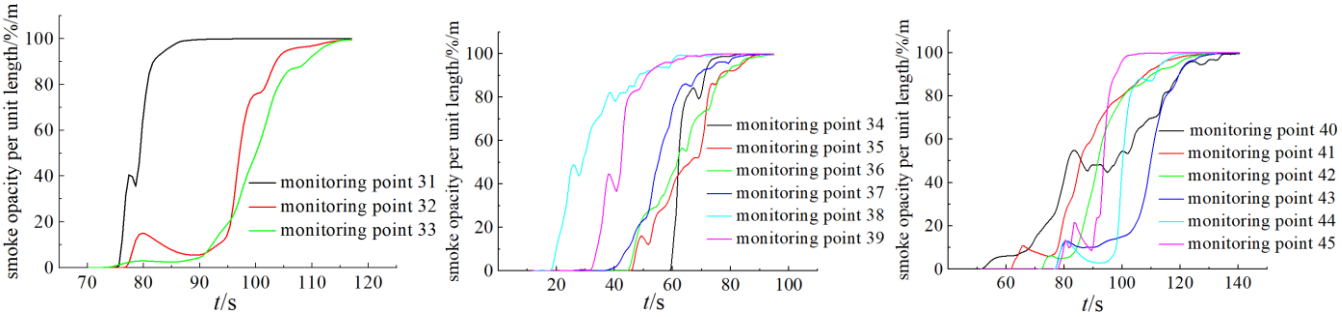

(a) First class (b) Business class (c) Luxury economy class

Figure 7. Smoke monitoring point data at z=3.6m in the upper cabin seats

The monitoring point for the height of human upright walking is at z=4.1 m, and the monitoring results are shown in fig. 8. In first class cabins, the speed of smoke propagation depends on the distance from the cabin head. In business class and luxury economy class, it depends on the distance from the ignition source. This pattern is different from when people bend down and move forward. In first class, business class, and luxury economy class, the shortest time for the smoke unit length opacity to increase to 100%/m is 88 s, 67 s, and 109 s, respectively. Under the condition of z=4.1 m altitude, the ranking of comprehensive danger level from low to high is luxury economy class, first class, and business class.

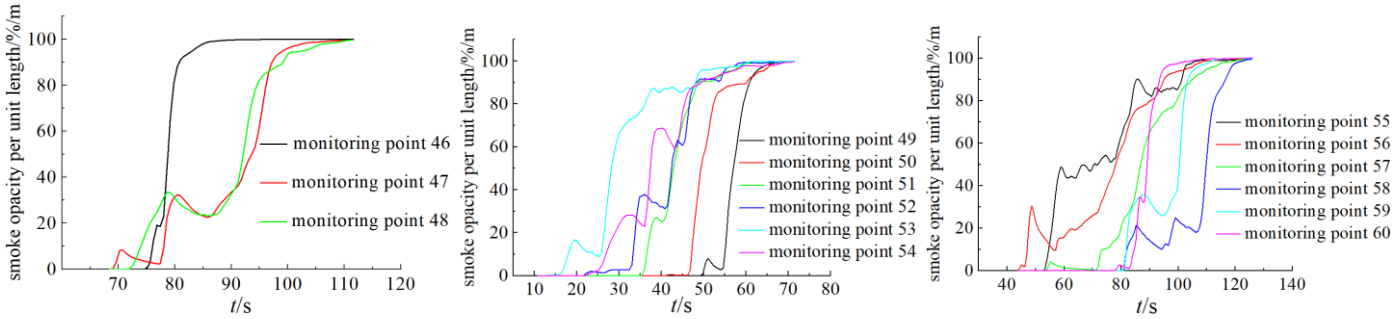

(a) First class (b) Business class (c) Luxury economy class

Figure 8. Smoke monitoring point data at z=4.1 m at the upper cabin seats

According to the data of upright walking and bending forward, it is found that smoke spreads faster at the height of the breathing belt during upright walking. Therefore, during evacuation, passengers sitting in the seat should bend down to escape in order to gain more escape time.

3.3. Temperature variation characteristics of fire in the upper cabin aisle

At the beginning of a fire, the spread of smoke is relatively stable. After a certain amount of smoke accumulates in a closed space, irregular vortices and entrainment phenomena will form, thereby accelerating the spread of temperature. The monitoring points with a breathing belt height of z=3.6 m are selected to study the temperature changes at the upper cabin aisle when a person bends down, as shown in fig. 9. The first class cabin remained unchanged after heating up to 95 ℃, with the highest temperature at monitoring point 61. The temperature of the business cabin remained unchanged after reaching 380 ℃, with the highest temperature observed at monitoring point 68. The luxury economy class remains unchanged after heating up to 90 ℃, with the highest temperatures observed at monitoring points 70 and 71. The closer the cabin is to the front of the first class cabin, the

higher the temperature, while the closer the business cabin is to the fire source, the higher the temperature. There is a significant difference in the highest temperature at a distance of less than 4 m from the fire source. The propagation speed of flame temperature is smaller than that of smoke.

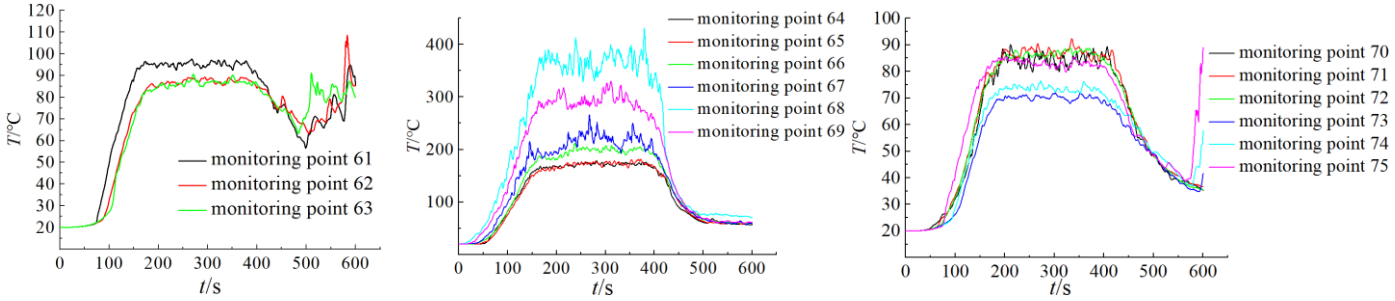

(a) First class (b) Business class (c) Luxury economy class

Figure 9. Temperature monitoring point data at z=3.6 m in the upper cabin aisle

The monitoring points with a breathing belt height of z=4.1 m are selected to study the temperature changes in the aisle during upright walking, as shown in fig. 10. At the height of the breathing belt during upright walking, the first class cabin remained unchanged after heating up to 110 ℃, and a flashover occurred at 500 s. The highest temperature was observed at monitoring point 78. The temperature of the business cabin remained unchanged after heating up to 440 ℃, with the highest temperature observed at monitoring point 83. The luxury economy class remained unchanged after heating up to 130 ℃, and a flashover occurred at 580 s, with the highest temperature observed at monitoring point 85. The closer the interior of first class, business class, and luxury economy class is to the source of fire, the higher the temperature. There is a significant difference in the highest temperature at a distance of less than 11 m from the fire source in the business cabin.

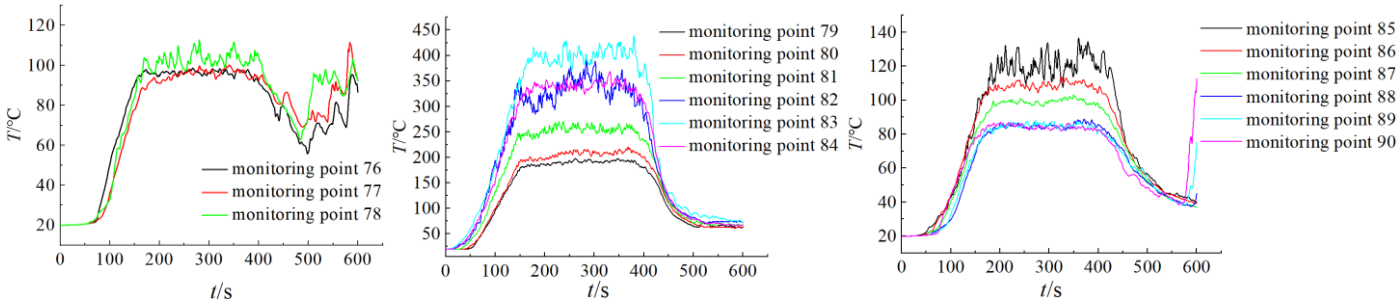

(a) First class (b) Business class (c) Luxury economy class

Figure 10. Temperature monitoring point data at z=4.1 m in the upper cabin aisle

3.4. Temperature variation characteristics of fire at the upper cabin seats

The monitoring points with a breathing belt height of z=3.6 m are selected to monitor the temperature changes at the upper cabin seats when the person bent forward, as shown in fig. 11. The first class cabin remained unchanged after heating up to 98 ℃, and a flashover occurred at 500 s, with the highest temperature observed at monitoring point 91. The temperature of the business cabin remained unchanged after heating up to 540 ℃, and the highest temperature was observed at monitoring point 98. The luxury economy class remained unchanged after heating up to 90 ℃, and a flashover occurred at 580 s. The highest temperatures were observed at monitoring points 100 and 101. In first class cabin, the temperature increases closer to the cabin head, while in business cabin, the

temperature increases closer to the fire source. There is a significant difference in the highest temperature at a distance of less than 4 m from the fire source.

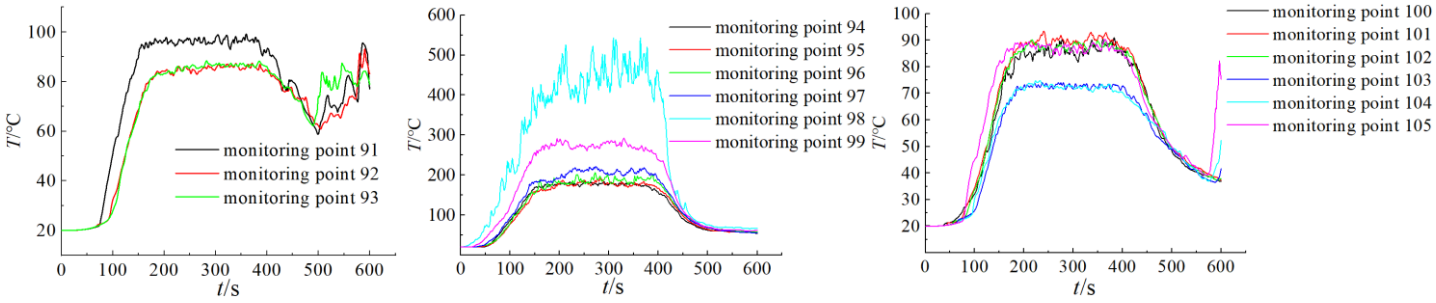

(a) First class (b) Business class (c) Luxury economy class

Figure 11. Temperature monitoring point data at z=3.6m in the upper cabin seats

When walking upright, the monitoring points with a breathing belt height of z=4.1 m is used to monitor the temperature at the upper cabin seats, as shown in fig. 12. The first class cabin remains unchanged after heating up to 100 ℃, and a flashover occurs at 500 s. The temperature of the business cabin remains unchanged after heating up to 500 ℃, with the highest temperature at monitoring point 113. The luxury economy class remained unchanged after heating up to 130 ℃, and a flashover occurred in 580 s, with the highest temperature at monitoring point 115. In first class, business class, and luxury economy class, the closer to the ignition source, the higher the temperature. Overall, at the same height, the temperature of the seat position is generally higher than that of the aisle position.

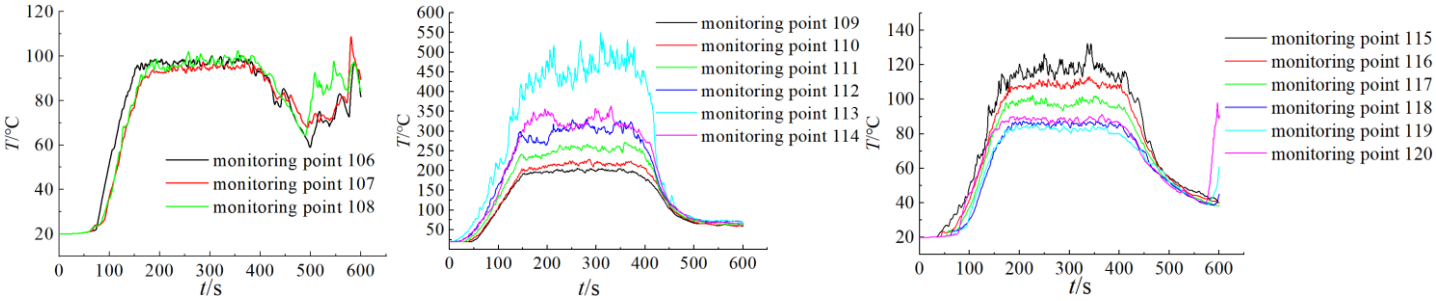

(a) First class (b) Business class (c) Luxury economy class

Figure 12. Temperature monitoring point data at z=4.1 m in the upper cabin seats

4. Conclusions

At z=3.6 m in the upper cabin aisle, smoke propagation in first class, business, and luxury economy cabins takes 89 s, 59 s, and 83 s, respectively. At z=4.1 m in the upper cabin aisle, the smoke propagation time is longer. At a height of 3.6 m in the upper cabin seats, smoke propagation in first class, business, and luxury economy cabins takes 89 s, 82 s, and 106 s. At z=4.1 m in the upper cabin seats, smoke propagation takes 88 s, 67 s, and 109 s.

At z=3.6 m in the upper cabin aisle, monitoring point 1 in first class cabin has the highest temperature, 8 in business cabin has the highest temperature, 10 and 11 in luxury economy cabin have the highest temperature. At z=4.1 m in the upper cabin aisle, the highest temperature monitoring points in first class, business class, and luxury economy class are 18, 23, and 25. At z=3.6 m in the upper cabin seats, the highest temperature monitoring points in first class, business class, and luxury economy class are 31, 38, and 40.

At z=4.1 m in the upper cabin seats, there is not much difference in temperature in the business cabin, with the highest temperature at monitoring point 53 and the highest temperature at monitoring point 55 in the luxury economy class. At the aisle and seat z=3.6 m in the upper cabin, the temperature in the first class cabin increases as it approaches the cabin head, while in the business cabin and luxury economy cabin, the temperature increases as it approaches the ignition source. At z=4.1 m in the upper cabin aisle and seats, the closer to the fire source, the higher the temperature in first class, business class, and luxury economy class.

Acknowledgment

The authors are grateful for the financial support provided by the Natural Science Foundation of China (12102271), and the Research Project of Education Department of Liaoning Province (JYTMS20230262).

References

[1] Payri, R., *et al.,* Parametrical Study of the Dispersion of An Alternative Fire Suppression Agent through A Real-size Extinguisher System Nozzle under Realistic Aircraft Cargo Cabin Conditions, *Process Saf. Environ., 141* (2020), pp. 110-122

[2] Chu, G. Q., *et al.,* Study on Probability Distribution of Fire Scenarios in Risk Assessment to Emergency Evacuation, *Reliab. Eng. Syst. Safe., 99* (2011), pp. 24-32

[3] Wang, J., *et al.,* Investigation on the CO Concentration Decay Profile and Spread Velocity of A Ceiling Jet at Reduced Pressure in Aircraft Cargo Compartment Fires, *Appl. Therm. Eng., 127* (2017), pp. 1246-1251

[4] Li, C., *et al.,* Influence of Depressurized Environment on the Fire Behaviour in a Dynamic Pressure Cabin, *Appl. Therm. Eng., 125* (2017), pp. 972-977

[5] Hu, L. H., *et al.,* Pool Fire Flame Base Drag Behavior with Cross Flow in A Sub-atmospheric Pressure, *P. Combust. Inst., 36* (2016), 2, pp. 3105-3112

[6] Hu, L. H., *et al.,* Flame Heights and Fraction of Stoichiometric Air Entrained for Rectangular Turbulent Jet Fires in A Sub-atmospheric Pressure, *P. Combust. Inst., 36* (2016), 2, pp. 2995-3002

[7] Feng, R., *et al.,* Experimental Study on the Burning Behavior and Combustion Toxicity of Corrugated Cartons under Varying Sub-atmospheric Pressure, *J. Hazard. Mater., 379* (2019) pp. 120785

[8] Tang, F., *et al.,* Mean Flame Height and Radiative Heat Flux Characteristic of Medium Scale Rectangular Thermal Buoyancy Source with Different Aspect Ratios in a Sub-atmospheric Pressure, *Int. J. Heat Mass Tran., 84* (2015) pp. 427-432

[9] Tang, F., *et al.,* Burning Rate and Flame Tilt Characteristics of Radiation-controlled Rectangular Hydrocarbon Pool Fires with Cross Air Flows in a Reduced Pressure, *Fuel, 139* (2015) pp. 18-25

[10] Liu, J. H., *et al.,* The Burning Behaviors of Pool Fire Flames under Low Pressure, *Fire Mater., 40* (2016), 2, pp. 318-334

[11] Lu, K. L., Experimental investigation on the suppression of aluminum dust explosion by sodium carbonate powder, *Process Saf. Environ., 183* (2024), pp. 568-579

[12] Zheng, K., Application of large eddy simulation in methane-air explosion prediction using thickening flame approach, *Process Saf. Environ., 159* (2022), pp. 662-673

[13] Cheng, Y. F., Hybrid H_2/Ti dust explosion hazards during the production of metal hydride TiH_2 in a closed vessel, Int. J. Hydrogen. Energ., *44* (2019), pp. 11145-11152

[14] Wang, W., *et al.*, Study of the Influence of Low Air Pressures on Fire Behavior and Burn-through of Aircraft Cargo Liner, *Fire Mater., 46* (2021), 5, pp. 789-796

[15] Wang, W., *et al.*, Investigation of the Effect of Low Pressure on Fire Hazard in Cargo Compartment, *Appl. Therm. Eng., 158* (2019), pp. 113775

[16] Papadogianni, V., *et al.*, Cone Calorimeter and Thermogravimetric Analysis of Glass Phenolic Composites Used in Aircraft Applications, *Fire Technol., 56* (2019), pp. 1253-1285

[17] Tranchard, *et al.*, Fire Behaviour of Carbon Fibre Epoxy Composite for Aircraft: Novel Test Bench and Experimental Study, *J. Fire Sci., 33* (2015), 3, pp. 247-266

[18] Maniccam, S., Effects of Back Step and Update Rule on Congestion of Mobile Objects, *Physica A, 346* (2005) pp. 631-650

[19] Miyoshi, T., *et al.*, An Emergency Aircraft Evacuation Simulation Considering Passenger Emotions, *Comput. Ind. Eng., 62* (2012), 3, pp. 746-754

[20] Nagatani, T., *et al.*, Statistical Characteristics of Evacuation without Visibility in Random Walk Model, *Physica A, 341* (2004) pp. 638-648

[21] Song, W. G., *et al.*, Simulation of Evacuation Processes Using a Multi-grid Model for Pedestrian Dynamics, *Physica A, 363* (2006), 2, pp. 492-500

[22] Tajima, Y., *et al.*, Scaling Behavior of Crowd Flow Outside a Hall, *Physica A, 292* (2001), 1, pp. 545-554

[23] Zheng, X. P., *et al.*, Forecasting Model for Pedestrian Distribution under Emergency Evacuation, *Reliab. Eng. Syst. Safe., 95* (2010), 11, pp. 1186-1192

[24] Qin, J. W., *et al.*, Simulation on Fire Emergency Evacuation in Special Subway Station Based on Pathfinder, *Case Stud. Therm. Eng.*, 21 (2020) pp. 100677

[25] Zhang, Z. M., *et al.*, Experiment and Modeling of Exit-selecting Behaviors During a Building Evacuation, *Physica A, 389* (2010), 4, pp. 815-824

[26] Zuo, Q. L., *et al.*, Simulation of Fire Smoke Disaster in a Goaf During the Closure Process, *Therm. Sci., 25* (2021), 5A, pp. 3399-3407

[27] Kuminecz, J. F., Full-scale flammability test data for validation of aircraft fire mathematical models, *NASA Technical Reports*, (1982) pp. 1-874

Submitted: 06.04.2024.
Revised: 29.06.2024.
Accepted: 30.06.2024.